12-30-2021

Self-Assembly of Black Cumin Oil-Based Nanoemulsion on Various Surfactants: A Molecular Dynamics Study

Aulia Fikri Hidayat
Department of Pharmacy, Faculty of Mathematics and Natural Sciences, Universitas Islam Bandung, Bandung 40116, Indonesia, aulia.fikri.h@unisba.ac.id

Taufik Muhammad Fakih
Department of Pharmacy, Faculty of Mathematics and Natural Sciences, Universitas Islam Bandung, Bandung 40116, Indonesia

Self-Assembly of Black Cumin Oil-Based Nanoemulsion on Various Surfactants: A Molecular Dynamics Study

Aulia Fikri Hidayat[*]and Taufik Muhammad Fakih

Department of Pharmacy, Faculty of Mathematics and Natural Sciences, Universitas Islam Bandung,
Bandung 40116, Indonesia

*E-mail: aulia.fikri.h@unisba.ac.id

Abstract

Black cumin is commonly used as traditional medicine due to its wide range of pharmacological potential. Black cumin oil (BCO) was often prepared as nanoemulsion to improve its solubility, stability, and bioavailability. This study was conducted to investigate the molecular behavior as well as structural evolution of BCO-surfactant systems during self-assembly micellization using molecular dynamics (MD) simulations. Several BCO constituents and variations of surfactants were employed to model BCO-surfactant systems. 50 ns of MD simulations were performed to elucidate their evolution of structures and physicochemical properties during formation. Results showed that BCO-tween20 and BCO-lecithin were able to form spherical-shaped micelles with the effective radii of 10.20 and 8.67 nm at the end of the simulation. Also, from the root mean square deviation and radius of gyration profile, it is showed that BCO-tween20 system was able to maintain the stability of its structure throughout the simulation. Results also revealed that self-assembly of BCO-surfactant systems were exothermic processes, confirming spontaneous nature upon formation.

Keywords: black cumin, micelles, molecular dynamics, nanoemulsion, self-assembly

Introduction

Black cumin (*Nigella sativa*) is a widely used natural product due to its vast pharmacological activities. Several reports showed its potential as antioxidant [1], antibacterial [2], anticancer [3], anti-inflammatory [4], and antidiabetic [5]. The beneficial effects of black cumin arise due to the presence of various constituents. Thymoquinone, thymohydroquinone, thymol, carvacrol, longifolene, *p*-cymene, 4-terpineol, and *t*-anethole [6] were present, along with fatty acids including linoleic acid, oleic acid, and palmitic acid [7,8].

In order to enhance its solubility, stability, and bioavailability, black cumin oil (BCO) was often formulated in the form of nanoemulsion [9]. Generally, fabrication method of nanoemulsion can be divided into high-energy methods and low-energy methods. In high-energy methods, particular instruments, like high-shear and high-pressure homogenizers, as well as ultrasonicators were required to generate molecular disruption [10]. Meanwhile, low-energy methods taking advantages of the internal energy of the system, promoting spontaneous emulsification when specific composition and condition are fulfilled [11]. A simple nanoemulsion is composed of water phase, oil phase, and surfactant(s) [9]. Surfactant plays an essential role in the formulation of nano-emulsion due to its ability in lowering interfacial tension in water-oil interface and inhibiting droplet coalescence [12]. Thus, a proper selection of surfactants is necessary to promote micellization and produce stable nanoemulsion.

Many experimental research have been conducted to investigate the formulation of BCO-based nanoemulsion. However, there is still lack of understanding in molecular details of self-assembly and micellization phenomena, as well as the physicochemical properties underlying the formation of nanoemulsion. Molecular dynamics (MD) simulation was considered as an appropriate technique to illustrate details of molecular interaction and behavior, as well as structural evolution during aggregation. MD simulations have been applied to study the self-assembly process of cyclohexane-based nanoemulsion [13], the molecular assembly of soybean oil-based nanoemulsion [14], the molecular aggregation of palm-based esters nanoemulsion [15,16], interaction between functionalized nanoparticles with lipid membranes [17], as well as dynamics of lecithin-encapsulated curcumin micelles [18]. In this study, the structural evolution and the physicochemical properties of BCO-surfactant systems in water environment during micellization process were examined. Several surfactant molecules were used to offer an insight on their performance in the formation of nanoemulsion.

Simulation Methods

From several research it was found that the major constituents in black cumin oil are fixed oils which comprised of 40-60% linoleic acid, 17-25% oleic acid, and 9-13% palmitic acid [1,7,8,19]. 0.4-2.5% of essential oils was also identified, with thymoquinone being its major component [7]. To model an efficient nanoemulsion system, a proportionate number of molecules, consist of 4 linoleic acid, 3 oleic acid, 2 palmitic acid, 1 thymoquinone, and 10 surfactant molecules were applied. Furthermore, in order to present an accurate understanding on the molecular behavior of BCO-surfactant system, several surfactants that have been employed in previous experimental studies were selected: tween20 (T20) [20], tween80 (T80), span20 (S20), span80 (S80) [21], and lecithin (LEC) [22].

Atom types of the BCOs and surfactant molecules were first prepared using PRODRG [23]. 10 BCO molecules and 10 surfactant molecules were then randomly placed in 10 nm × 10 nm × 10 nm simulation box using PACKMOL [24]. Simulation processes were carried out using GROMACS 2021 [25]. The GROMOS96 force field [26] was applied for BCOs and surfactants, while spc216 model was used for water. The steepest descent and leapfrog algorithm were performed during 500,000 steps of energy minimization converging its value below 50 kJ/mol.nm.

The minimized system was then equilibrated under canonical (NVT; constant number of molecules, volume, and temperature) ensemble for 500 ps until reference temperature was reached at 310 K, continued by equilibration under isothermal-isobaric (NPT; constant number of molecules, pressure, and temperature) ensemble for the same duration until 1 bar of reference pressure and 310 K of reference temperature were set. Molecular dynamics production step was then performed in isothermal-isobaric ensemble for 50 ns with the integrating step of 2 fs. Both Particle Mesh Ewald (PME) and van der Waals forces were set at cut-off value of 1.4 nm in order to handle electrostatic and short-range interaction, respectively. Modified Berendsen thermostat [27] and Parrinello-Rahman barostat [28] were employed for temperature and pressure coupling during simulation. Visualization of structure evolution was observed using visual molecular dynamics (VMD) software [29]. Root mean square deviation (RMSD), radius of gyration, and several physicochemical properties were calculated using GROMACS modules. These steps were repeated in the same manner for all surfactant molecules.

Results and Discussion

Prior to MD production step, the BCO-surfactant systems were equilibrated for 500 ps under NVT and NPT ensembles, consecutively. Potential energy profiles during both equilibrations are showed in Figure 1. NVT phase equilibration was conducted to ensure that the desired temperature of the system is reached, and fixed during the remainder of the simulation. It is showed that the potential energy of five BCO-surfactant systems plateaued after 50 ps, indicating that the systems were canonically equilibrated. The NPT phase was then performed, to stabilize the pressure of the system, as well as its density. It is indicated from the graph that the potential energies of all systems are fluctuated. However, it should be noticed that the fluctuating values are confined in the trendlines of each system. Thus, it is safe to assume that each BCO-surfactant system was generally equilibrated under isothermal-isobaric condition.

In the MD production phase, BCO and surfactant molecules were initially placed in random fashion and underwent structural evolution in five simulations as shown in Figure 2 (a) – (e). At 25 ns of simulation, the molecules were assembled, showing aggregation toward micelle-like structures. A single cluster structure was occurred in BCO/T20 system. Similar structures were also found in BCO/T80, BCO/S20, and BCO/LEC, although they possess different characteristics. In BCO/T80, two monomer clusters were formed, while one spherical micelle-like and a smaller monomer cluster were present in BCO/S20 system. It can also be observed that BCO/LEC system formed an almost-cylindrical structure along with a single monomer. In the end of simulation at 50 ns, molecules position in
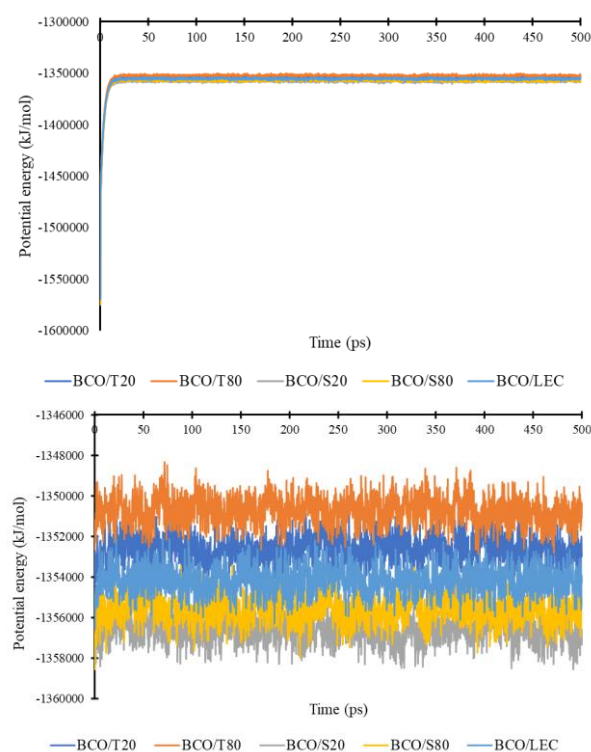
Figure 1. Potential Energy Profiles during NVT (Above) and NPT Equilibration (Below)
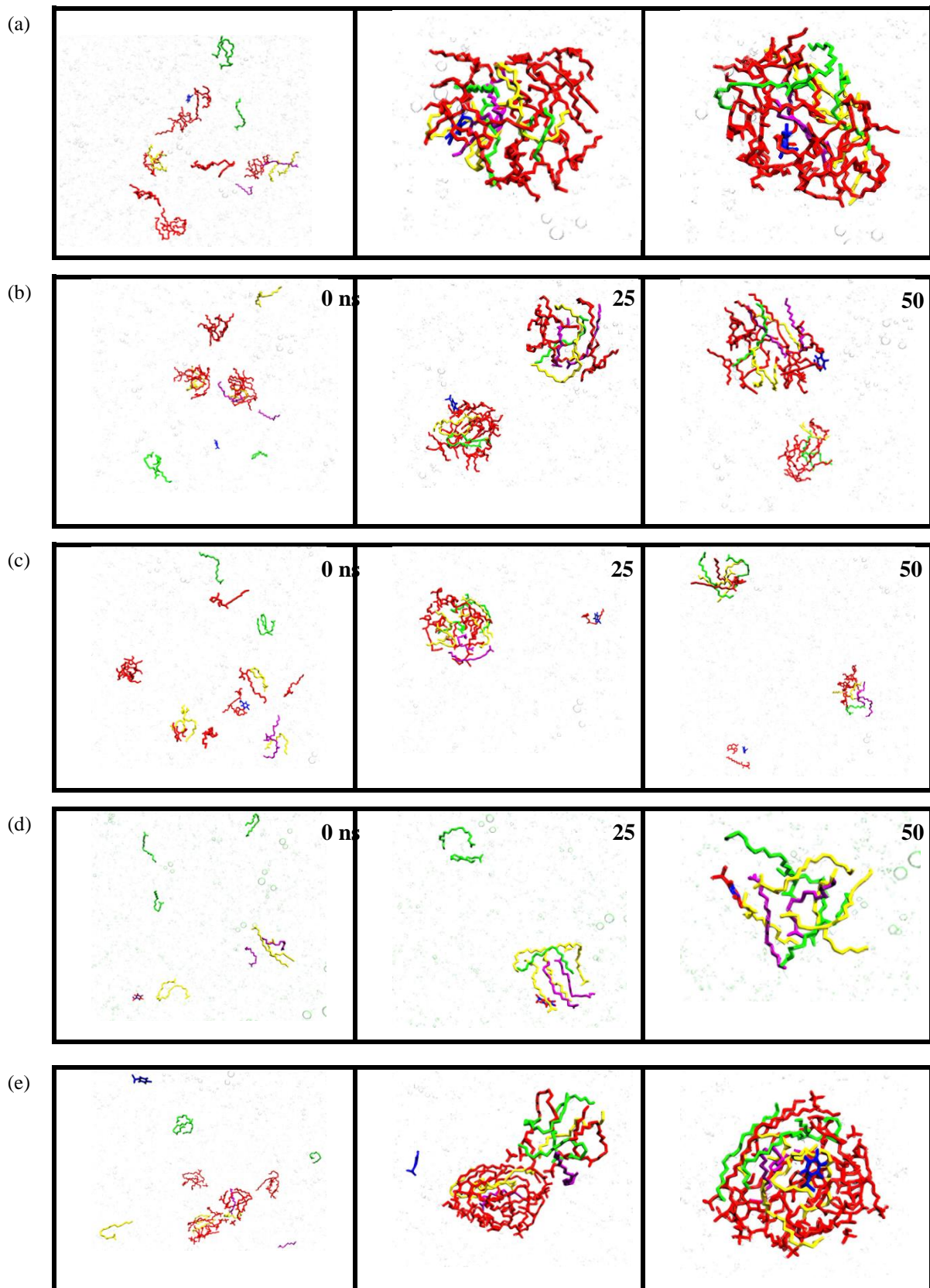
Figure 2.   Snapshots (Zoomed-in According to Cluster Area) during Simulation from 0 to 50 ns of: (a) BCO/T20, (b) BCO/T80, (c) BCO/S20, (d) BCO/S80, and (e) BCO/LEC. Color-represented Molecules: Surfactants (red), Thymoquinone (blue), Linoleic Acid (yellow), Oleic Acid (Green), Palmitic Acid (Purple)

BCO/T20 was rearranged while still maintaining the stability of its micelle shape. BCO/T80 molecules also repositioned in a similar manner. The structure of BCO/S20, however, broken apart at the final structure, separated into several cluster of monomers, indicating span20 inability to perform micellization. In BCO/S80 system, one cluster of free monomers was formed without the indication of micelle shape structure. The inability of span20 and span80 to form micelles illustrated in this study also confirming previous experimental result, in which BCO microemulsion was failed to obtain when span20 and span80 were applied as surfactants [21]. On the other hand, a significantly different result was found to occur in BCO/LEC system. The molecules were reassembled toward a single spherical micelle, with the lecithin positioned on the outermost layer of the structure, encapsulating BCO constituents inside the system.

In order to further the comprehension towards the molecular behavior and structural evolution during micelle formation, root mean square deviation (RMSD) in five simulations were calculated. In the context of biomolecular simulation, RMSD is a statistical-based quantity that describes displacement of specific atoms in a molecule relative to a reference structure using least-square fitting method [30].

The RMSD of BCO-surfactant systems is shown in Figure 3. During first 10 ns of simulation, the RMSD of all systems showing steep increases. This is due to frequent movement of the molecules in their effort to reach equilibrium states. After 10 ns, noticeably different profiles were shown. Until the end of simulation BCO/T20 system showed a relatively more stable state than the other systems, indicating only small changes occurred in the position of atoms in the structure. More fluctuating behavior were shown in BCO/T80, BCO/S20, BCO/S80, and BCO/LEC systems. This showed that these systems were more unstable due to frequently repositioned atoms during simulation. From the RMSD of BCO-surfactant in five systems, it can be concluded that tween20 was able to aid spontaneous formation of a stable micelle during nano-emulsification process.

Throughout the simulation process, evolution of structure compactness was also occurred. Radius of gyration (*Rg*) can be calculated to explain this phenomenon. *Rg* is defined as the distance of a point inside concentrated mass of a system from the axis of rotation [31]. When applied, this specific radius would maintain the moment inertia around the axis [32].

Rg of BCO-surfactant systems is shown in Figure 4. From the graph it is showed that BCO/T20 underwent two steep climbs at 0 – 4 ns and 9 – 11 ns. Shortly after 11 ns until the end of simulation this system has reached equilibrium, which also evident from its snapshot (Figure 2a) and RMSD graph (Figure 3). This is indicating that

tween20 were able to maintain the compactness of molecules aggregate without any significant structural changes. This result also confirmed previous experimental study that showed the capability of tween20 in forming a stable and homogeneous submicron-emulsion of black cumin oil [20]. Similar to the RMSD, *Rg* profiles of BCO/T80 and BCO/S80 were heavily fluctuating, showing multiple structural changes during formation. On the other hand, although forming a singular micelle shape in the final structure, a mild fluctuation was present in the *Rg* of BCO/LEC. This means that BCO/LEC structure is subject to change if longer simulation is conducted. It was reported that the amount of lecithin is related to the emulsifying capacity and emulsion stability [22]. Emulsifying capacity determine the emulsification ability of a surfactant. At certain amount, addition of lecithin improving the emulsifying capacity, while lowering the stability of its BCO emulsion system. Thus, it can be assumed that despite the ability of lecithin to perform micellization, structural changes in BCO-lecithin system might still be occurred in the long run. Furthermore, by closely looking the RMSD and *Rg* profiles of BCO/S20, an interesting case was found.
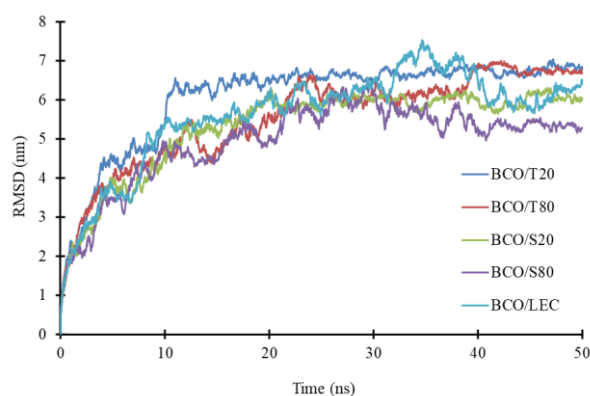
Figure 3. RMSD of All Systems during Simulation
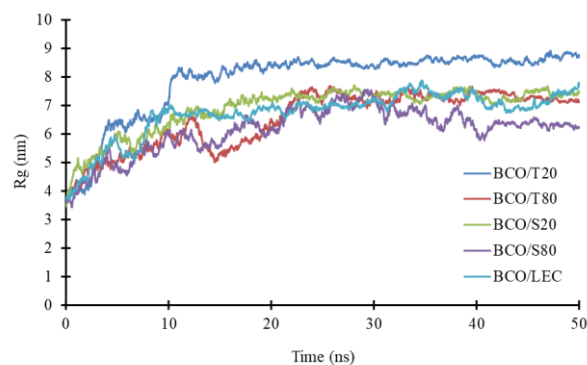
Figure 4. Radius of Gyration of All Systems during Simulation

Table 1. Physicochemical Properties of BCO-surfactant Systems

System	Potential Energy ($\times 10^6$) (kJ/mol)	Enthalpy ($\times 10^6$) (kJ/mol)	#Surf*SurfTen (bar nm)
BCO/T20	-1.354	-1.111	0.975
BCO/T80	-1.352	-1.109	-0.520
BCO/S20	-1.357	-1.115	-2.073
BCO/S80	-1.357	-1.114	-0.245
BCO/LEC	-1.355	-1.113	4.212

Although micelle shape was not formed at the end of simulation, this system was less fluctuated than BCO/T80, BCO/S80, and BCO/LEC systems. This is possibly due to the quasi-equilibrium states during structural changes, i.e., when morphologies change more rapidly than clusters collisions, so that the clusters are considered as several subsystems [33].

From the average radius of gyration, the effective radius (*Rs*) of an oil-surfactant droplet can be estimated using $Rs = \sqrt{5/3}\langle Rg \rangle$ [34]. However, this equation may be valid when spherical shape was assumed [35]. Based on the assumption of BCO-surfactants spherical micelles at the final simulation, only *Rs* of BCO/T20 and BCO/LEC was calculated, obtaining effective radii of 10.20 and 8.67 nm, respectively.

To gain more understanding toward physicochemical characteristics in the formation of BCO-surfactants nanoemulsion, several quantities were calculated. This calculation was performed using gmx energy module from GROMACS. Average values of potential energy, enthalpy, and number of surfaces multiplied by surface tension of five systems are shown in Table 1.

The potential energy in a system of molecules can be defined as the sum of bonded and non-bonded interactions. Bond length, angles, and dihedral angles are contributing in bonded interactions which respectively describe stretching, bending, and torsions of atoms in the system. Meanwhile, the non-bonded interactions are present due to van der Waals and electrostatic interactions, which generally described by Lennard-Jones potential and Coulomb potential, respectively [36]. From Table 1, it is showed that the calculated average potential energy of five systems were not greatly differ. This indicates that despite the difference of structures, all contributing interactions were uniformly distributed for all systems.

In molecular self-assembly, constituent molecules are spontaneously rearranging themselves to form a specific structure without the necessity of external energies. During self-assembly formation of BCO-surfactant structures, negative values of average enthalpy were found in all systems. This showed the characteristic of energy-releasing exothermic process upon micellization [37]. Furthermore, the enthalpy-driven process that occurs in our systems may be due to electrostatic repulsion in the hydrophilic part of the surfactants [38].

Interesting results were found in the calculation of number of surfaces multiplied by surface tension (#Surf*SurfTen). In isothermal-isobaric ensemble, surface tension is dependent on the normal pressure, lateral pressure in *x*- and *y*-axis, and the average value of half the box length in *z*-axis [39]. In our result, average negative values were found in the BCO/T80, BCO/S20, and BCO/S80 systems. Assuming the number of surfaces (or interfaces) were always positive, the negative signs were contributed from the surface (or interfacial) tension. This is possibly due to computational consequences, in which the calculated interacting forces were dependent on their directions. In addition, the negative values of surface/interfacial tension also have been discussed in several studies, converging similar arguments that negative surface/interfacial tension may appear in a non-equilibrium condition due to rapid interfacial reaction [40] as well as strong repulsion between components in the system of emulsion [41].

Conclusion

Self-assembly formation of black cumin oil-based nanoemulsion was investigated using molecular dynamics simulations. The MD simulation was performed by selecting several black cumin oil constituents and various surfactants in aqueous environment. Structure evolution during production until the end of simulation showed different surfactant capabilities in micellization process. Spherical micelles were formed in the end of simulation when tween20 and lecithin were applied, with the effective radii of 10.20 and 8.67 nm, respectively. However, a stable configuration was occurred only in BCO-tween20 system. It can also be concluded that spontaneous self-assembly of BCO nanoemulsion was an exothermic process in nature.

References

[1] Solati, Z., Baharin, B.S., Bagheri, H. 2014. Antioxidant property, thymoquinone content and chemical characteristics of different extracts from *Nigella sativa* L. seeds. J. Am. Oil Chem. Soc. 91(2): 295–300, https://doi.org/10.1007/s11746-01 3-2362-5.

[2] Bourgou, S., Pichette, A., Marzouk, B., Legault, J. 2012. Antioxidant, anti-inflammatory, anticancer and antibacterial activities of extracts from *nigella sativa* (black cumin) plant parts. J. Food. Biochem. 36(5): 539–546, https://doi.org/10.1111/j.1745-451 4.2011.00567.x.

[3] Agbaria, R., Gabarin, A., Dahan, A., Ben-Shabat, S. 2015. Anticancer activity of *Nigella sativa* (black seed) and its relationship with the thermal processing and quinone composition of the seed. Drug Des. Devel. Ther. 9: 3119–3124, https://doi.o rg/10.2147/DDDT.S82938.

[4] Khader, M., Eckl, P.M. Thymoquinone: An emerging natural drug with a wide range of medical applications. 2014. Iran J. Basic Med. Sci. 17(12): 950–957, doi:10.22038/ijbms.2015.3851.

[5] Mathur, M.L, Gaur, J., Sharma, R., Haldiya, K.R. Antidiabetic Properties of a Spice Plant *Nigella sativa*. 2011. J. End. Metab. 1(1): 1–8, https://doi.org/10.4021/jem12e.

[6] Randhawa, M.A., Alghamdi, M.S. Anticancer activity of *Nigella sativa* (Black Seed) - A review. 2011. Am. J. Chin. Med. 39(6): 1075–1091, https://doi.org/10.1142/S0192415X1100941X.

[7] Ghahramanloo, K.H., Kamalidehghan, B., Akbari Javar, H., Teguh Widodo, R., Majidzadeh, K., Noordin, M.I. 2017. Comparative analysis of essential oil composition of iranian and indian *nigella sativa* L. Extracted using supercritical fluid extraction and solvent extraction. Drug. Des. Devel. Ther. 11: 2221–2226, https://doi.org/10.2147/DD DT.S87251.

[8] Işık, S., Aslan Erdem, S., Kartal, M. 2019. Investigation the fatty acid profile of commercial black cumin seed oils and seed oil capsules: Application to real samples. J. Chem. Metrol. 13(2): 53–60, https://doi.org/10.25135/jcm.26.19.0 8.1385.

[9] Mohammed, N.K., Muhialdin, B.J., Meor Hussin, A.S. 2020. Characterization of nanoemulsion of *Nigella sativa* oil and its application in ice cream. Food Sci. Nutr. 8(6): 2608–2618, https://doi.org/1 0.1002/fsn3.1500.

[10] McClements, D.J., Rao, J. 2011. Food-Grade nanoemulsions: Formulation, fabrication, properties, performance, Biological fate, and Potential Toxicity. Crit. Rev. Food Sci. Nutr. 51(4): 285–330, https://doi.org/10.1080/10408398.2011.559558.

[11] Solans, C., Solé, I. 2012. Nano-emulsions: Formation by low-energy methods. Curr. Opin. Coll. Inter. Sci. 17(5): 246–254, https://doi.org/10.1 016/j.cocis.2012.07.003.

[12] Uluata, S., Decker, E.A., McClements, D.J. 2016. Optimization of Nanoemulsion Fabrication Using Microfluidization: Role of Surfactant Concentration on Formation and Stability. Food Biophys. 11(1): 52–59, https://doi.org/10.1007/s11483-015-9416-1.

[13] Pirhadi, S., Amani, A. 2020. Molecular dynamics simulation of self-assembly in a nanoemulsion system. Chem. Pap. 74(8): 2443–2448, https://doi.o rg/10.1007/s11696-020-01050-3.

[14] Moghaddasi, F., Housaindokht, M.R., Darroudi. M., Bozorgmehr, M.R., Sadeghi, A. 2018. Soybean oil-based nanoemulsion systems in absence and presence of curcumin: Molecular dynamics simulation approach. J. Mol. Liq. 264: 242–252, https://doi.org/10.1016/j.molliq.2018.05.066.

[15] Abdul Rahman, M.B., Huan, Q.Y., Tejo, B.A., Basri, M., Salleh, A.B., Rahman, R.N.Z.A. 2009. Self-assembly formation of palm-based esters nano-emulsion: A molecular dynamics study. Chem. Phys. Lett. 480(4–6): 220–224, https://doi.org/10.1016/j.c plett.2009.08.073.

[16] Karjiban, R.A., Huan, Q.Y., Abdul Rahman, M.B., Basri, M., Tejo, B.A. 2015. Self-assembly of Palm Kernel Oil Wax Esters in Aqueous Media: A Molecular Dynamics Study. Int. J. Chem. 7(1): 133, https://doi.org/10.5539/ijc.v7n1p133.

[17] Das, M., Dahal, U., Mesele, O., Liang, D., Cui, Q. 2019. Molecular Dynamics Simulation of Interaction between Functionalized Nanoparticles with Lipid Membranes: Analysis of Coarse-Grained Models. J. Phys. Chem. B. 123(49): 10547–10561, https://doi.org/10.1021/acs.jpcb.9b0 8259.

[18] Hakim, L., Mardiana, D., Rokhiyah, U., Lestari, M.L.A.D., Ningsih, Z. 2021. Structure and Dynamics of Curcumin Encapsulated Lecithin Micelles : A Molecular Dynamics Simulation Study. Sci. Technol. Indones. 6(3): 113–120, https://doi.org/10.26554/sti.2021.6.3.113–120.

[19] Yimer, E.M., Tuem, K.B., Karim, A., Ur-rehman, N., Anwar, F. 2019. *Nigella sativa* L. (Black Cumin): A Promising Natural Remedy for Wide Range of Illnesses. Evidence-Based Complement. Altern. Med. 2019: 1–16.

[20] Shaaban, H.A., Sadek, Z., Edris, A.E., Saad-Hussein, A. 2015. Analysis and antibacterial activity of *nigella sativa* essential oil formulated in microemulsion system. J. Oleo. Sci. 64(2): 223–232, https://doi.org/10.5650/jos.ess14177.

[21] Mohd Nor, N.H., Mohd Shafri, M.A., Mohamed, F. 2014. Preparation and characterization of *Nigella*

sativa microemulsions. Int. J. Pharm. Pharm. Sci. 6: 485–489.

[22] Varlı, M., Solak, R., Turan, S., Ramadan, M.F. 2021. Physical characteristics of black cumin oil emulsions compared to sunflower and corn oils emulsions. J. Food Meas. Charact. 15: 3207–3215, https://doi.org/10.1007/s11694-021-00900-2.

[23] Van Aalten, D.M.F. 1996. PRODRG, a program for generating molecular topologies and unique molecular descriptors from coordinates of small molecules. J. Comput. Aided Mol. Des. 10(3): 255–262, https://doi.org/10.1007/BF00355047.

[24] Martinez, L., Andrade, R., Birgin, E.G., Martinez, J.M. 2009. Packmol: A Package for Building Initial Configurations for Molecular Dynamics Simulations. J. Comput. Chem. 30(13): 2157–2164, https://doi.org/10.1002/jcc.

[25] Van Der Spoel, D., Lindahl, E., Hess, B., Groenhof, G., Mark, A.E., Berendsen, H.J.C. 2005. GROMACS: Fast, flexible, and free. J. Comput. Chem. 26(16): 1701–1718, https://doi.org/10.1002/jcc.20291.

[26] Bonvin, A.M.J.J., Mark, A.E., Van Gunsteren, W.F. 2000. GROMOS96 benchmarks for molecular simulation. Comput. Phys. Commun. 128(3): 550–557, https://doi.org/10.1016/S0010-4655(99)00540-8.

[27] Berendsen H.J.C., Postma, J.P.M., Van Gunsteren, W.F., Dinola, A., Haak, J.R. 1984. Molecular dynamics with coupling to an external bath. J. Chem. Phys. 81(8): 3684–3690, https://doi.org/10.1063/1.448118.

[28] Parrinello, M., Rahman, A. 1981. Polymorphic transitions in single crystals: A new molecular dynamics method. J. Appl. Phys. 52(12): 7182–7190, https://doi.org/10.1063/1.328693.

[29] Humphrey, W., Dalke, A., Schulten, K. 1996. VMD: Visual Molecular Dynamics. J. Mol. Graph. 14: 33–38.

[30] Cheng, Y., Yuan, S. 2020. Emulsification of Surfactant on Oil Droplets by Molecular Dynamics Simulation. Mol. 25(3008): 1–15, https://doi.org/10.3390/molecules25133008.

[31] Pirhadi, S., Amani, A. 2020. Molecular dynamics simulation of siRNA loading into a nanoemulsion as a potential carrier. J. Mol. Model. 26(8), https://doi.org/10.1007/s00894-020-04471-9.

[32] Ma, J., Song, X., Peng, B. 2021. Multiscale molecular dynamics simulation study of polyoxyethylated alcohols self-assembly in

emulsion systems. Chem. Eng. Sci. 231: 116252, https://doi.org/10.1016/j.ces.2020.116252.

[33] Hagan, M.F., Elrad, O.M., Jack, R.L. 2011. Mechanisms of kinetic trapping in self-assembly and phase transformation. J. Chem. Phys. 135(10): 1–13, https://doi.org/10.1063/1.3635775.

[34] Wei, Y., Wang, H., Liu, G., Wang, Z., Yuan, S. 2016. A molecular dynamics study on two promising green surfactant micelles of choline dodecyl sulfate and laurate. RSC Adv. 6(87): 84090–84097, https://doi.org/10.1039/c6ra16536b.

[35] Karjiban, R.A., Basri, M., Rahman, M.B.A., Salleh, A.B. 2012. Structural Properties of Nonionic Tween80 Micelle in Water Elucidated by Molecular Dynamics Simulation. APCBEE Proc. 3(May): 287–297, https://doi.org/10.1016/j.apcbe.2012.06.084.

[36] De Vivo, M., Masetti, M., Bottegoni, G., Cavalli, A. 2016. Role of Molecular Dynamics and Related Methods in Drug Discovery. J. Med. Chem. 59(9): 4035–4061, https://doi.org/10.1021/acs.jmedchem.5b01684.

[37] Hoque, M.A., Mahbub, S., Rub, M.A., Rana, S., Khan, M.A. 2018. Experimental and theoretical investigation of micellization behavior of sodium dodecyl sulfate with cetyltrimethylammonium bromide in aqueous/urea solution at various temperatures. Korean J. Chem. Eng. 35(11): 2269–2282, https://doi.org/10.1007/s11814-018-0120-y.

[38] Flores-Andrade, E., Allende-Baltazar, Z., Sandoval-González, P.E., Jiménez-Fernández, M., Beristain, C.I., Pascual-Pineda, L.A. 2021. Carotenoid nanoemulsions stabilized by natural emulsifiers: Whey protein, gum Arabic, and soy lecithin. J. Food Eng. 290, https://doi.org/10.1016/j.jfoodeng.2020.110208.

[39] Chandrasekhar, I., Bakowies, D., Glättli, A., Hünenberger, P., Pereira, C., Van Gunsteren, W.F. 2005. Molecular dynamics simulation of lipid bilayers with GROMOS96: Application of surface tension. Mol. Simul. 31(8): 543–548, https://doi.org/10.1080/08927020500134243.

[40] Patashinski, A.Z., Orlik, R., Paclawski, K., Ratner, M.A., Grzybowski, B.A. 2012. The unstable and expanding interface between reacting liquids: Theoretical interpretation of negative surface tension. Soft Matter. 8(5): 1601–1608, https://doi.org/10.1039/c1sm06590d.

[41] Kaptay, G. 2017. On the negative surface tension of solutions and on spontaneous emulsification. Langmuir. 33(40): 10550–10560, https://doi.org/10.1021/acs.langmuir.7b01968.